Original article DOI: 10.2478/aiht-2022-73-3608

Effects of naringin and valproate interaction on liver steatosis and dyslipidaemia parameters in male C57BL6 mice

David Jutrić[1,2], Domagoj Đikić[1], Almoš Boroš[1], Dyna Odeh[1], Sandra Domjanić Drozdek[3], Romana Gračan[1], Petar Dragičević[4], Irena Crnić[5], and Irena Landeka Jurčević[5]

[1] University of Zagreb Faculty of Science, Zagreb, Croatia
[2] Clinical Hospital Dubrava, Zagreb, Croatia
[3] University of Applied Health Sciences, Zagreb, Croatia
[4] University of Zagreb School of Medicine, Zagreb Croatia
[5] University of Zagreb Faculty of Food Technology and Biotechnology, Zagreb, Croatia

[Received in October 2021; Similarity Check in November 2021; Accepted in February 2022]

Valproate is a common antiepileptic drug whose adverse effects include liver steatosis and dyslipidaemia. The aim of our study was to see how natural flavonoid antioxidant naringin would interact with valproate and attenuate these adverse effects. For this reason we treated male C57BL6 mice with a combination of 150 mg/kg of valproate and 25 mg/kg naringin every day for 10 days and compared their serum triglycerides, cholesterol, LDL, HDL, VLDL, and liver PPAR-alpha, PGC-1 alpha, ACOX1, Nrf2, SOD, CAT, GSH, and histological signs of steatosis. Valproate increased lipid peroxidation parameters and caused pronounced microvesicular steatosis throughout the hepatic lobule in all acinar zones, but naringin co-administration limited steatosis to the lobule periphery. In addition, it nearly restored total serum cholesterol, LDL, and triglycerides and liver ACOX1 and MDA to control levels. and upregulated PPAR-alpha and PGC-1 alpha, otherwise severely downregulated by valproate. It also increased SOD activity. All these findings suggest that naringin modulates key lipid metabolism regulators and should further be investigated in this model, either alone or combined with other lipid regulating drugs or molecules.

KEY WORDS: ACOX1; cholesterol; dyslipidaemia; lipid regulating transcription factors; Nrf2; oxidative stress; PPAR-alpha; PGC-1 alpha

Valproic acid (di-n-propylacetic acid, 2-propylpentanoic acid, 2-propylvaleric acid) is a branched short-chain fatty acid first synthesised by alkylation of valeric acid originating from the plant *Valeriana officinalis*. The acid and its derivative valproate is used to treat epilepsy, neuropsychiatric disorders, and some oncological and infectious diseases. Its primary mode of action is to inhibit histone deacetylases in cells. However, prolonged use or overdosing may lead to serious adverse effects (1–5). These occur when serum concentrations rise above 200 mg/L and include hyper- or hypothermia, tachycardia, and hypotension. Higher concentrations can lead to coma, respiratory arrest, asystole, and death (3–5). With chronic use, main adverse effects include nephrotoxicity (Fanconi's syndrome) and hepatotoxicity associated with metabolic disorders, dyslipidaemia in particular (3–5). In subchronic dosing, the conjugates of 2,4-diene valproate and coenzyme A (CoA) may disturb several pathways in the beta-lipid oxidation cascade and cholesterol synthesis in the liver causing liver steatosis and lipid accumulation (1–6).

Several animal model studies have shown, however, that many natural bioactive compounds and molecules, including naringin (5–9), can attenuate or even reverse some of these effects if given with other substances (8) and valproate (5–7, 9). Naringin (4,5,7-trihydroxy flavanone-7-rhamnoglucoside) is a polyphenolic compound derived from citrus plants with antioxidative, anti-inflammatory, anti-apoptotic, and lipid-lowering action (8–10). It was shown to lower oxidative stress by upregulating nuclear factor erythroid 2-related factor 2 (NFE2R2 aka Nrf2), to downregulate proinflammatory mediators such as tumour necrosis factor alpha (TNF-alpha), cyclooxygenase-2 (COX-2), and inducible NO synthase by inhibiting nuclear factor kappa B (NF-$\varkappa$B), and to upregulate the Farnesoid X receptor (FXR), a ligand-activated transcription factor involved in the expression of various proteins and biosynthetic enzymes essential for the physiological maintenance of cholesterol and the expression of liver fatty acid-binding protein (L-FABP) (11). In many models investigating hepatotoxicity it was shown to modulate steatosis, necrosis, hydropic degeneration, and congestion in liver injury (10, 11).

We therefore wanted to evaluate how the combined use of valproate and naringin would affect some of the lipid metabolism and oxidative stress parameters in the liver in the *in vivo* model, as research has been limited to *in vitro* effects so far (10).

Corresponding author: Domagoj Đikić, University of Zagreb Faculty of Science, Department of Animal Physiology, Biology Division, Rooseveltov trg 6, 10000 Zagreb, Croatia, E-mail: *domagoj.djikic@biol.pmf.hr*, ORCID: 0000-0003-0909-3488

MATERIALS AND METHODS

Experimental animals and treatment

A total of 24 male inbred C57BL/6 mice, weighing 30±1.5 g, were obtained from the University of Zagreb Faculty of Science Department of Animal Physiology. Animals had free access to standard laboratory diet (4 RF 21, Mucedola Srl, Settimo Milanese, Italy) and tap water and were kept under the 12/12 hour light cycle, in line with standard housing conditions for laboratory mice (12), and the experiments were approved by the Bioethics Committee of the Zagreb University Faculty of Science (Approval No: 251-58-10617-17-7).

Animals were randomly divided into four groups (six per group): control, valproate, naringin, and valproate + naringin group. The control group was receiving saline. The valproate group was receiving 150 mg of valproate/valproic acid (Depakine®, Sanofi, Carbon Blanc, France) per kg of body weight (bw). Naringin (Sigma-Aldrich, St. Louis, MO, USA) was administered in the dose of 25 mg/kg bw. The combination group was receiving the same doses of each compound. The rationale for the valproate dose was to simulate overdosing with approximately three times higher therapeutic dose (4). As for naringin, we estimated the dose from previous reports (8, 10, 11). Each compound was administered daily as a 0.2 mL water solution by gavage for 10 days between 8 and 10 a.m. to avoid differences in metabolism related to the circadian rhythm.

On day 11, 24 h after the animals received the last, 10th dose, they were anaesthetised with isoflurane (3 % in O_2 flow 0.8–1.5 L/min) and injected with a mix of 100 mg/kg ketamine and 10 mg/kg xylazine.

Tissue preparation

Blood was collected by cardiac puncture, and animals sacrificed by cervical dislocation. Collected blood was centrifuged to isolate serum for biochemical parameters. Serum was immediately frozen at -80 °C until analysis. Livers were isolated and parts of tissue samples placed in 50 mmol/L phosphate-buffered saline (PBS, pH=7.4) and homogenised (10 % of homogenate by tissue mass per volume of PBS) with an ultrasonic homogeniser (SONOPLUS HD2070, BANDELIN electronic, Berlin Germany) using an MS73 probe (BANDELIN). The homogenates were then sonicated on ice for 30 s in three 10-second intervals and centrifuged at 4 °C and 20000×g for 15 min and immediately frozen at -80 °C until the analysis of oxidative stress parameters and transcription factors. Small liver samples for histological examination were frozen without any chemical treatment immediately after dissection and used for cryostat histology.

Serum lipids and serum biochemistry

Lipids were analysed with the Beckman Coulter OSR61118 kit, total cholesterol with the OSR6216 kit, and HDL cholesterol with OSR6195 (Beckman Coulter, Brea, CA, USA) according to manufacturer instructions. Chromophore reactions were analysed on a Tecan Infinite 200 plate reader (Tecan Group Ltd., Männedorf, Switzerland) at wavelengths recommended in kit instructions for each parameter with the coefficient of variation of up to 5 %. LDL cholesterol concentrations were calculated using the Friedewald equation (13, 14):

LDL-C=total cholesterol-HDL-C-[total tryglicerides/5]

Serum biochemistry

Serum biochemical parameters were analysed on a VetScan™ VS2 device with a Comprehensive Diagnostic Profile reagent rotor (Zoetis, Parsippany, NJ, USA) according to manufacturer instructions.

Histology of lipid deposits in the liver

Oil red O (CAS 1320-06-5) histological dye was obtained from Sigma-Aldrich and applied to frozen liver sections (15 μm) following the protocol for lipid and fat staining described below. The working solution was prepared with 0.5 % Oil Red O in propylene glycol (Sigma-Aldrich). The slides were air-dried at room temperature for 30 min and then fixed in ice cold 10 % formaldehyde (Biognost, Zagreb, Croatia) for 10 min, and rinsed with running tap and then distilled water. The slides were immersed into Oil Red O working solution for 10 min, rinsed twice with distilled water, counterstained with haematoxylin M (Biognost) for 5 s, rinsed thoroughly with tap and then distilled water for 3 min, and mounted with glycerine jelly. Three slides per animal were evaluated and photographed with a Nikon Eclipse E600 light microscope (Nikon, Tokyo, Japan) equipped with an AxioCam ERc5s digital camera and a ZEN2 lite software (Carl Zeiss Microscopy Deutchland, Oberkochen, Germany) at 100× magnification (15).

Liver PPAR-alpha, PGC1-alpha, ACOX1, and Nrf2 assays

To measure the levels of peroxisome proliferator-activated receptor alpha (PPAR-alpha), peroxisome proliferator-activated receptor gamma coactivator 1-alpha (PPARGC1A, aka PGC-1 alpha), acyl-coenzyme A oxidase 1 (ACOX1) activity, and Nrf2 in mouse liver tissue homogenates we used corresponding microwell strip plate enzyme-linked immunosorbent assay (ELISA) kits (MyBioSource Inc., San Diego, CA, USA, catalogue Nos. MBS2502542, MBS707053, MBS9316691, and MBS744301, respectively) according to manufacturer instructions. Colour intensity for all three kits was measured on a Tecan Infinite 200 microplate reader.

Liver oxidative stress analysis

Frozen tissue supernatants as described above were slowly thawed on +6 °C cooling pads until they became liquid again. They

were then centrifuged at 4 °C and 20000×*g* for 15 min and used to analyse markers of oxidative stress as described below.

Protein concentrations in liver tissue homogenates express all biochemical and molecular parameters as units per mg of protein and were determined according to Lowry et al. (16), with bovine serum albumin (BSA) as the standard.

Lipid peroxidation was determined by measuring malondialdehyde (MDA) using a modified method described by Landeka Jurčević et al. (17). A 200 μL sample of centrifuged homogenised tissue was mixed with 200 μL of 8.1 % sodium dodecyl sulphate (SDS), 1.5 mL of 20 % acetic acid (pH=3.5), and 1.5 mL of 0.81 % thiobarbituric acid and incubated at 95 °C for 60 min. After cooling on ice, the absorbance was measured at 532 and 600 nm with a Libro S22 ultraviolet-visible (UV-Vis) spectrophotometer (Biochrom Ltd. Cambridge, UK). Total absorbance was determined by deducting absorbance at 600 nm from the absorbance measured at 532 nm. MDA levels were then determined using the molar extinction coefficient for malondialdehyde-thiobarbiturate (MDA–TBA) complex of 1.56×10^5 L/mol cm and expressed as nmol/mg of protein in tissue homogenate.

Carbonylated proteins in the liver were determined by adding 200 μL of sample homogenate to 300 μL of 10 mmol/L 2,4-dinitrophenylhydrazine (DNPH) in 2 mol/L HCl and shaking at room temperature for 1 h. Proteins were precipitated with 10 % (w/v) trichloroacetic acid (TCA) at -20 °C for 5 min and then centrifuged at 4 °C and 12000x*g* for 10 min. The supernatant was removed and the precipitate resuspended in a 1:1 mixture of ethanol and ethyl acetate and centrifuged under the same conditions. The obtained pellet was washed repeatedly until all unbound DNPH was removed. The residue was then dissolved in 6 mol/L guanidine HCl at 35 °C. The resulting solution was used to measure absorbance at λ=370 nm. Carbonylated protein concentration was calculated using the molar extinction coefficient 22,000 L/mol cm and expressed as nmol/mg protein (19).

Superoxide dismutase (SOD) activity was determined as described previously by Landeka Jurčević et al. (17). Briefly, an undiluted sample of tissue homogenate (25 μL) was mixed with 1.45 mL of reaction solution [0.05 mmol/L of cytochrome C and 1 mmol/L of xanthin mixed with 5,5'-dithiobis(2-nitrobenzoic acid) (DTNB) in the 10:1 (v/v) ratio]. This mixture was added 20 μL of xantine oxidase (0.4 U/mL) to start the reaction. The absorbance was measured with the UV-Vis spectrophotometer mentioned above at 550 nm for 3 min. One unit of SOD activity was defined as the amount of enzyme required to inhibit 50 % of superoxide anion production within the sample. The results were expressed as units per mg of protein in tissue homogenate (U/mg protein).

Liver catalase (CAT) activity was assayed by measuring the initial rate of hydrogen peroxide degradation as described by Landeka Jurčević et al. (17). The reaction mixture was prepared by mixing 33 mmol/L H_2O_2 in 50 mmol/L phosphate buffer (pH=7.0). This reaction mixture (900 μL) was mixed with tissue supernatant (100 μL), and the absorbance measured with the UV-Vis spectrophotometer at 240 nm for 3 min. CAT activity was calculated using the molar extinction coefficient of 43.6 L/mol cm for H_2O_2. The results were expressed as U/mg protein.

Reduced glutathione (GSH) determination has been described earlier by Landeka Jurčević et al. (17). Briefly, 40 μL of 10 mmol/L DTNB was added to each well of a 96-well plate containing 20 μL of tissue supernatant (obtained as described above) pre-treated with 40 μL of 350 mmol/L HCL and incubated for 10 min. Then we added 100 μL of reaction solution prepared earlier by mixing 9980 μL of 0.8 mmol/L nicotinamide adenine dinucleotide phosphate (NADPH) and 20 μL of 0.2 U/mL glutathione reductase and read absorbance at 412 nm for 5 min in an ELISA plate reader (Biorad Laboratories, Hercules CA, USA). GSH levels were determined from calibration curve of GSH standards. The results are expressed as μmol/mg protein.

Statistical analysis

All the data are expressed as means ± standard deviations (SD). GraphPad Prism 9 (GraphPad Software, San Diego, CA, USA) was used for data analysis and statistical comparisons between the groups with Kruskal-Wallis and Tukey's test. The level of significance was set to $p<0.05$.

RESULTS

Serum lipid values

Figure 1 shows that valproate alone significantly increased ($p<0.05$) serum triglycerides and total cholesterol (Figure 1B), and naringin alone significantly increased ($p<0.05$) serum triglycerides compared to control, but their combination restored lipid levels to nearly normal.

Valproate alone did not affect lipoprotein levels (Figure 1C–E), while naringin added to valproate significantly reduced LDL ($p<0.05$) compared to the valproate group but not to control. In combined treatment lipoprotein levels did not significantly differ from control.

Serum biochemistry

Valproate also significantly increased serum glucose, creatinine, and bound urea nitrogen and amylase and lactate dehydrogenase activity compared to control ($p<0.05$) (Table 1), whereas naringin only increased glucose and lactate dehydrogenase activity significantly.

In combined treatment, however, it did not attenuate valproate effects, as the above parameters remained elevated. Interestingly, glucose and creatinine levels were even higher ($p<0.05$) in the combination group than in the valproate group.

Liver markers of lipid metabolism

In the liver tissue the Oil Red O method revealed that microvascular steatosis was the most pronounced in the valproate

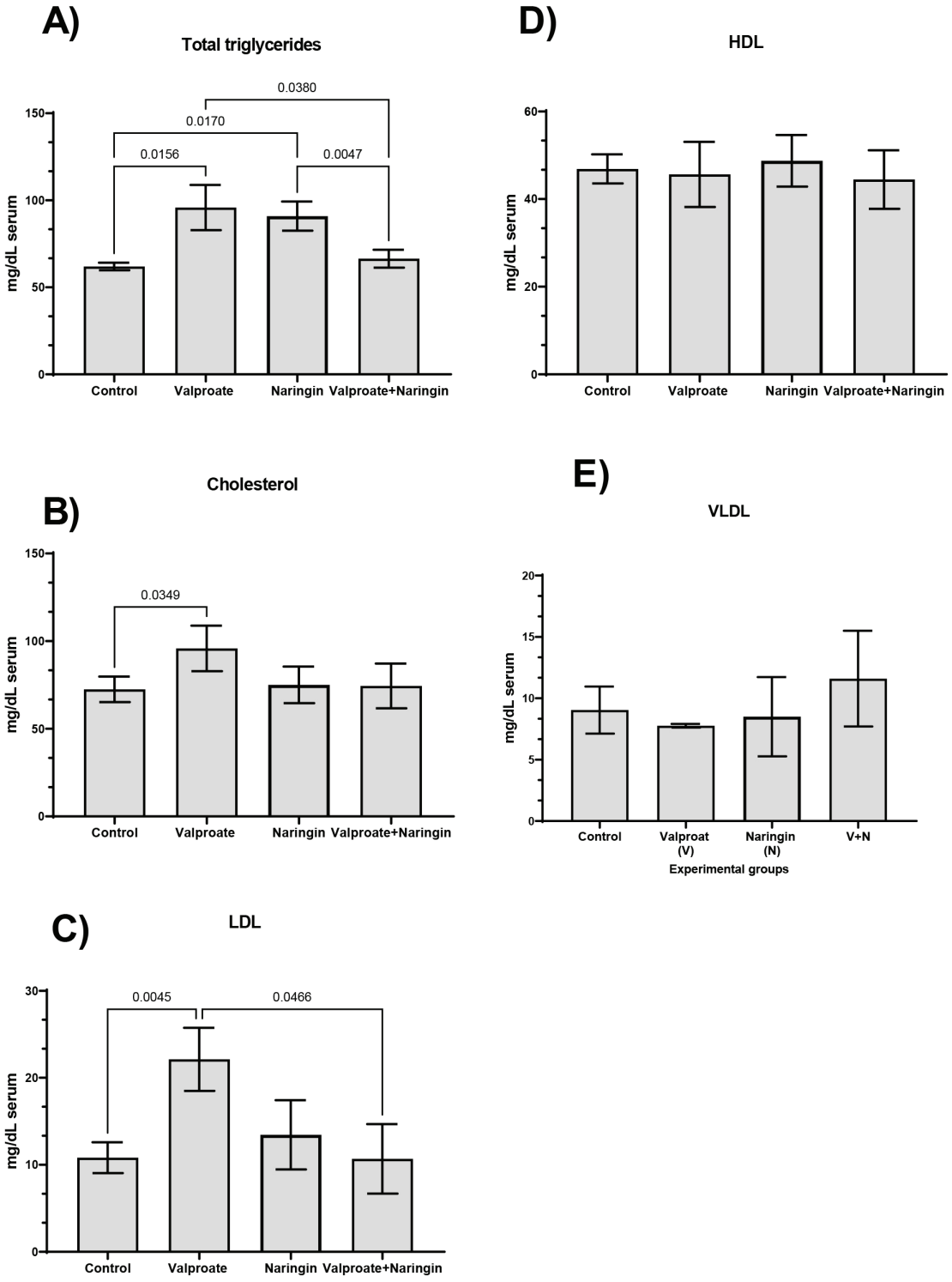

Figure 1 Serum lipids and lipoproteins in control mice and mice treated with daily doses of 150 mg/kg bw valproate, 25 mg/kg bw naringin, and their combination for 10 days. The numbers above bars represent statistically significant differences ($p<0.05$) between specific groups

Table 1 Serum biochemistry parameters in control mice and mice treated with daily doses of 150 mg/kg bw valproate, 25 mg/kg bw naringin, and their combination for 10 days

Parameter	Control	Valproate	Naringin	Valproate+Naringin
Glucose (mmol/L)				
Mean ± SD	5.9±0.9	**12.7±1.4**[a]	**14.0±4.2**[a,b]	**17.8±1.5**[b]
Median	5.8	12.6	13.4	16.3
Range	5.0–7.2	11.5–14.3	9.8–19.3	9.8–19.9
Amylase activity (U/L)				
Mean ± SD	365.3±110.6	**555.0±520.4**[a]	371.8±23.8	**455.8±102.4**[b]
Median	331.0	355.0	373.5	459.0
Range	273.0–526.0	184.0–1326.0	342.0–398.0	356.0–549.0
Lactate dehydrogenase (LDH) activity (U/L)				
Mean ± SD	264.8±29.2	**316.4±40.3**[a]	**382.0±97.8**[a]	**498.5±324.2**[a]
Median	257.0	331.0	392.0	531.5
Range	240.0–305.0	250.0–348.0	263.0–518.0	122.0–809.0
Creatinine (mg/L)				
Mean ± SD	22.8±3.3	**31.3±7.8**[a]	27.5±10.5	**42.8±3.6**[b]
Median	22.5	29.0	25.0	43.0
Range	19.0–27.0	25.0–42.0	18.0–42.0	24.0–56.0
Bound urea nitrogen (BUN) (mmol/L)				
Mean ± SD	6.0±1.3	**10.2±7.6**[a]	6.9±1.1	**10.0±3.4**[a]
Median	5.7	8.5	7.0	8.5
Range	4.8–7.7	3.0–21.0	5.4–8.0	7.9–15.0
Bilirubin (μmol/L)				
Mean ± SD	5.3±0.2	5.6±0.4	5.1±0.2	5.1±0.2
Median	5.3	5.8	5.0	5.1
Range	5.0–5.5	5.1–5.9	5.0–5.4	5.0–5.4
Alkaline phosphatase (ALP) activity (U/L)				
Mean ± SD	46.3±6.3	44.5±3.1	32.0±14.1	42.0±2.2
Median	47.3	45.5	38.5	41.5
Range	40.0–55.0	40.0–47.0	11.0–40.0	40.0–45.0
Total proteins (mg/L)				
Mean ± SD	37.3±5.0	34.5±10.2	40.5±5.9	38.1±0.9
Median	37.5	37.5	40.0	38.0
Range	32.0–42.0	20.0–43.0	37.0–49.0	37.0–39.0
Albumin (mg/L)				
Mean ± SD	27.0±2.4	34.3±6.5	36.0±5.0	31.0±0.8
Median	26.5	36.0	36.0	30.0
Range	25.0–30.0	25.0–40.0	30.0–42.0	29.0–33.0

[a,b] values marked with a superscript letters differ significantly from control; different letters mark significant differences the treatment groups ($p<0.05$). ALP – alkaline phosphatase; BUN – bound urea nitrogen; LDH – lactate dehydrogenase

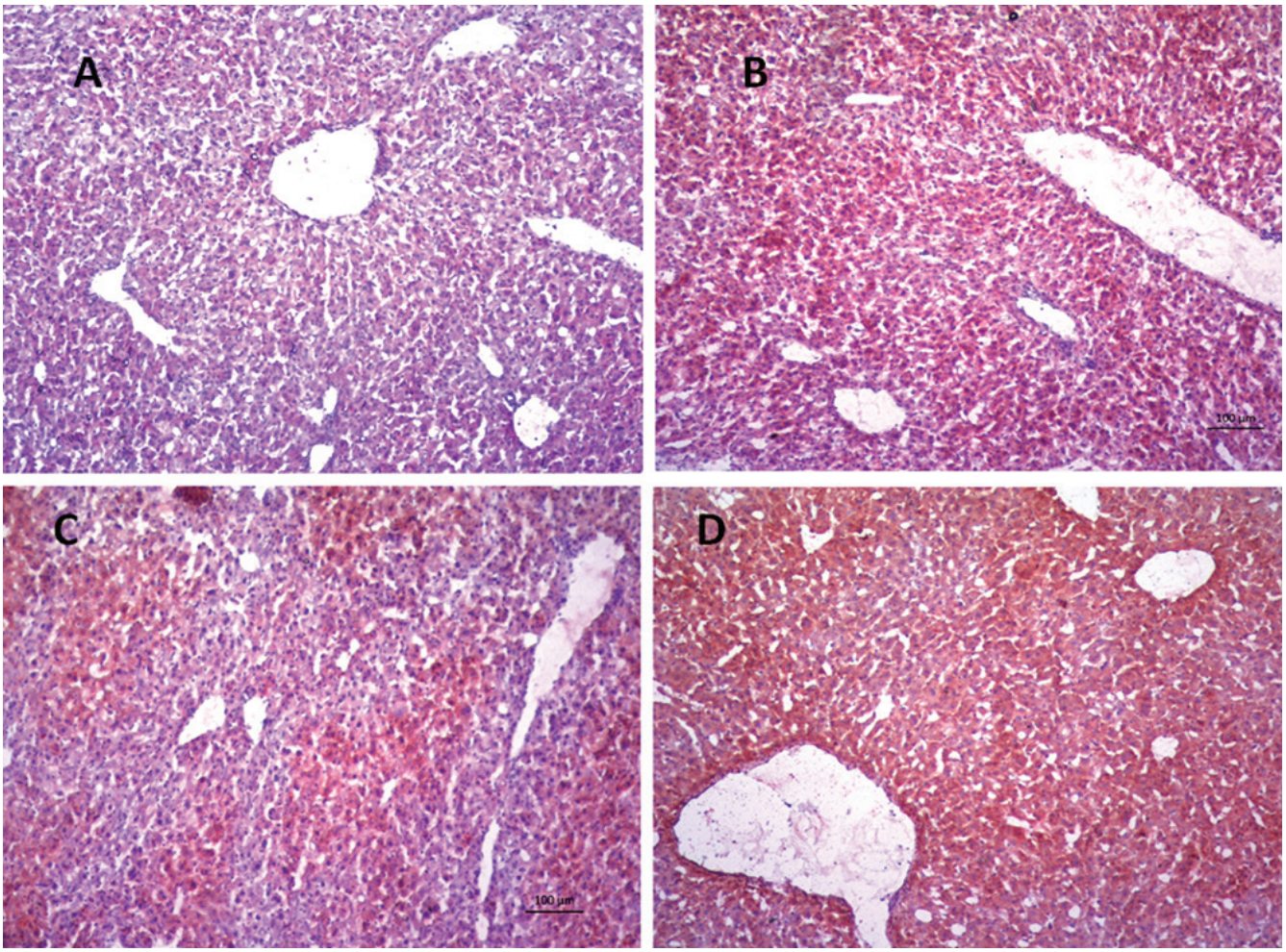

Figure 2 Lipid steatosis stained with Oil Red in the liver of control mice (A) and mice treated with daily doses of 150 mg/kg bw valproate (B), 25 mg/kg bw naringin (C), and their combination (D) for 10 days

group. In the combination group it was somewhat reduced, although still present (Figure 2). The difference was that hepatic steatosis in the valproate group spread all along the hepatic lobule in both the portal/central and peripheral zones, while lipid accumulation in the naringin group was limited to the acinus and lobule periphery.

Valproate significantly reduced the levels of transcription factors PPAR-alpha and PGC-1 alpha, which regulate lipid metabolism, while naringin annulled this effect in combined treatment, restoring these levels to control (Figure 3A and 3B).

Similar effect of naringin was observed with ACOX1, which was significantly increased by valproate and restored to control values in combined treatment (Figure 3C).

Liver oxidative stress markers

Valproate nearly doubled malondialdehyde (MDA), and naringin successfully countered this effect and restored its levels to control in combined treatment (Figure 4A). Judging by carbonylated protein levels, however, proteins were not damaged by oxidative stress in any of the treated groups (Figure 4B).

Compared to control, valproate did not significantly affect antioxidative defence markers SOD and CAT but significantly lowered GSH (Figure 5). Naringin, in turn, significantly increased SOD, but did not influence CAT or GSH. Combined treatment kept all three markers around control levels, although it is interesting to note higher GSH (Figure 5C), even though both valproate and naringin applied separately lowered its levels.

The transcription factor Nrf2, indicative of oxidative stress, showed no significant variations between treatments.

DISCUSSION

Our findings of valproate adverse effects on lipid metabolism support earlier reports in many aspects, from lipid accumulation and liver steatosis (3, 19–21) to a variety of mechanisms of action,

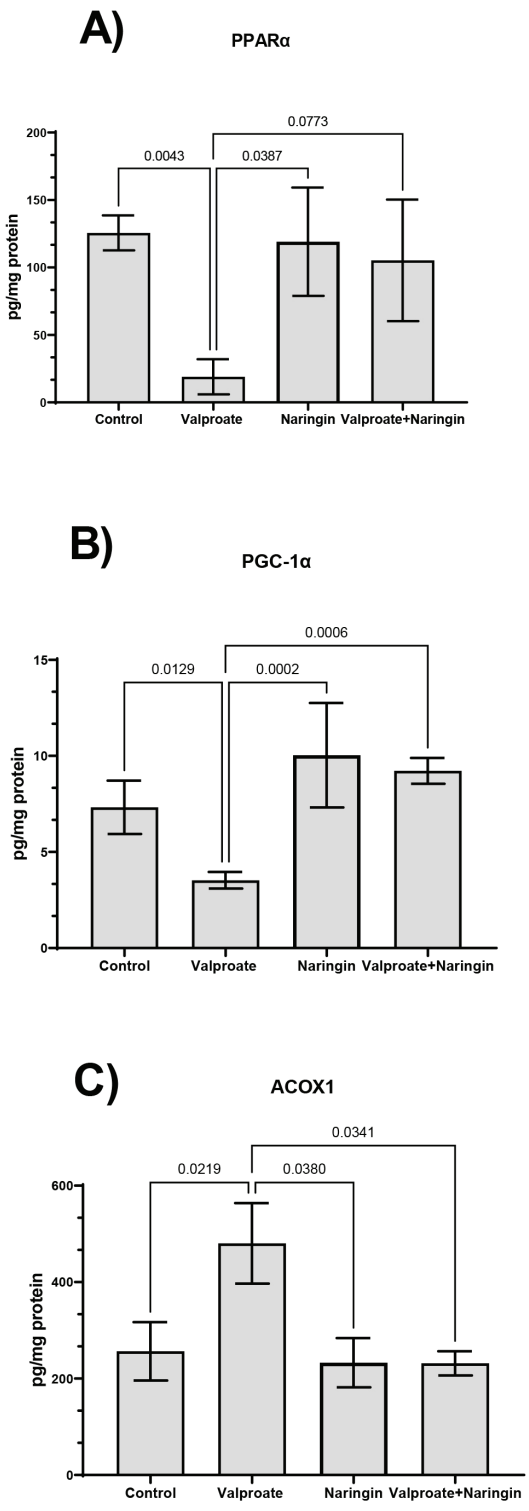

Figure 3 Liver lipid metabolism regulators in control mice and mice treated with daily doses of 150 mg/kg bw valproate, 25 mg/kg bw naringin, and their combination for 10 days. The numbers above bars represent statistically significant differences ($p<0.05$) between specific groups

including the inhibition and alteration of mitochondrial fatty acid beta oxidation or modulation of at least 60 genes involved in lipid metabolism (22–25).

Naringin combined with valproate, in turn, lowered serum and liver lipids compared to valproate treatment. Naringin is known to downregulate triglyceride cellular transporters, namely fatty acid binding protein (FABP1) and CD36 in hepatocytes (10, 19, 25) and to lower plasma cholesterol by inhibiting hepatic HMG-CoA reductase activity (26).

These effects could be associated with changes in PPAR-alpha and PGC-1 alpha levels determined in our study, as these transcription factors regulate fatty acid metabolism in mitochondria (27, 28). When highly expressed and activated in the cells their action decrease triglyceride levels and increase HDL (27–30). This could explain why we observed significantly lowered PPAR-alpha and PGC-1 alpha in our experiment and the increase in liver and serum lipids, as the lack of these transcription factors may have impaired lipid degradation by mitochondrial beta-oxidation (28, 29). These parameters were not disturbed in the naringin group and were restored to control levels in the group receiving the valproate and naringin combination, which seems to have attenuated lipid accumulation observed in the valproate group. Previously, *in vitro*, Zhang et al. (10) showed that naringin significantly reduced intracellular triglyceride accumulation (by 52.7 %) in liver tissue through its specific binding to CD36 and PPAR-alpha. They also showed that naringin highly increased PPAR-alpha content in lipid-rich liver. Our *in vivo* findings of PPAR-alpha support Zhang's *in vitro* report, as PPAR-alpha did not change under naringin treatment alone (normal conditions) but was restored to normal by naringin from values lowered by valproate in combined treatment. Similarly, upregulation of PGC-1 alpha by only 25 % has been shown to improve mitochondrial biogenesis and induce fatty acid oxidation (25, 29). Since it was significantly lower in the valproate group, this may explain fat accumulation. Naringin, in turn, has shown the opposite effect (Figure 3B).

Considering that peroxisome oxidation involves ACOX1 activity and that it entirely depends on PPAR-alpha (28, 30, 31), we expected that valproate-induced decrease in PPAR-alpha would entail a decrease in ACOX1 as well. Instead, our findings showed a significant ACOX1 increase in the valproate group. We looked for recent studies that would explain this phenomenon and the interplay between decreased PPAR-alpha and increased ACOX1 but could not find any. There are but a few early reports (31–33) of similar effects regarding this increase in ACOX1. Aoyama et al. (33) reported that PPAR-alpha-null mice (mice that have no PPAR-alpha in the body) had normal levels of ACOX, which suggests that ACOX1 does not necessarily and immediately decrease with the decrease or lack of liver PPAR-alpha when valproate is applied. In terms of our experiment, this could mean that although PPAR-alpha dropped, ACOX1 did not necessarily follow in its footsteps. ACOX in peroxisomes seems to remain highly active and oxidise valproic metabolites in peroxysomes. Earlier studies imply (34–36) that

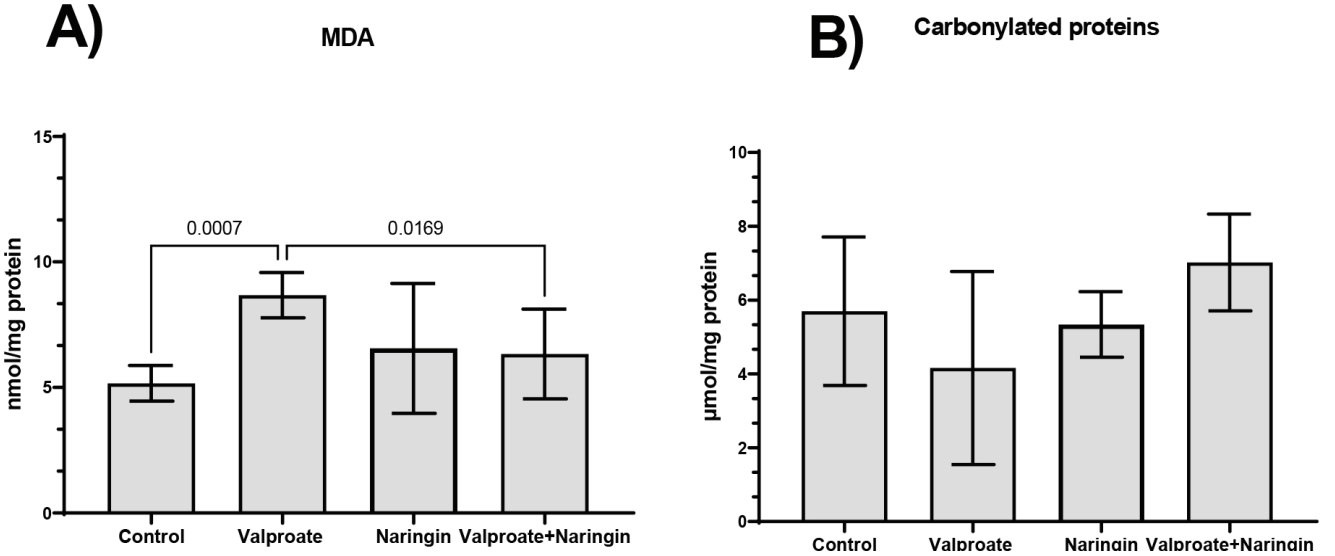

Figure 4 Liver tissue oxidative stress parameters in control mice and mice treated with daily doses of 150 mg/kg bw valproate, 25 mg/kg bw naringin, and their combination for 10 days. The numbers above bars represent statistically significant differences ($p<0.05$) between specific groups. MDA – malondialdehyde

valproate can, in fact, induce peroxisome proliferation and the activity of peroxisomal ACOX enzymes, including ACOX1, as demonstrated by our results here. Furthermore, this could mean that peroxisomes and perhaps their enzymes for lipid oxidation partially take over impaired mitochondrial oxidative function (30, 34, 36–38). Obviously, the valproate/PPAR-alpha/ACOX1 balance is rather complex, and there are probably other important molecular regulators and factors (such as sirtuin and the retinoid X receptor) that influence this interaction in the hepatocyte (30, 38–40). Future experiments should therefore address PPAR-alpha/ACOX1 temporal dynamics and other molecular components (39, 40) known to regulate the interaction between PPAR-alpha and ACOX1 transcription and peroxysomal activation.

In view of the above, our findings suggest that adding naringin to valproate may have restored lipid metabolism to normal levels by restoring the balance between ACOX1 and PPAR-alpha (41, 42). The observed increase in ACOX1 in our valproate group could certainly be connected to and probably is one of the causes of increased oxidative stress (MDA levels), because ACOX1 is known to produce hydrogen peroxide (43). Several authors (44–46) reported higher reactive oxygen species (ROS) and lower mitochondrial membrane potential in liver cells treated with valproate. Naringin added to valproate, in turn, reduced MDA significantly in comparison to the valproate group (Figure 4) and increased SOD. This action and normalisation of ACOX1 expression are probably its major mechanisms for reducing oxidative stress and lipid damage. This assumption is supported by rat study reports of naringin preventing inflammation, apoptosis, autophagy, and oxidative DNA damage by increasing SOD activity and thereby decreasing proinflammatory cytokines (9, 11, 44). In addition, naringin was reported to have significantly increased SOD, CAT, and GSH in the liver of LDL receptor knockout mice (26). The lowering of GSH levels in the valproate group in our study, however, could be the result of consumption by hydrogen peroxide produced due to higher ACOX1 activity.

As for liver injury markers (Table 1), unlike Köroğlu et al. (9), we found no significant variations in ALP levels between the groups. This may be due to interspecies differences (mice vs rats), about four times lower doses applied (150 vs 500 mg/kg of valproate and 25 vs 100 mg/kg of naringin) and shorter treatment duration (10 vs 14 days) in our study. Syed et al. (11) also applied four times higher naringin doses (100 mg/kg day) for eight weeks and observed complete absence of steatosis. By simple extrapolation, our 25 mg/kg naringin dose corresponds to a 1750 mg intake by a 70-kg person, which is a realistic dose for humans (like the dose found in food supplements), while Syed's dose corresponds to and unrealistic intake of 7,000 mg (7 g) for a 70-kg person. Jung et al. (47) reported that a 400 mg naringin capsule per day taken for eight weeks reduced serum cholesterol in hypercholesteraemic subjects by 14 % and LDL cholesterol by 17 % but did not have any effect in healthy controls. Demonty et al. (48), in turn, reported no naringin effects in hypercholesteraemic subjects at 500 mg a day over four weeks. In our experiment, serum triglyceride even increased in the naringin group and liver histology showed a slight accumulation of lipids compared to control. Combined with valproate, it did not completely resolve liver steatosis but rather diminished and limited it to acinar outskirts. We could therefore partly agree with Köroğlu et al. (9) that naringin does not completely protect against the adverse effects of valproate.

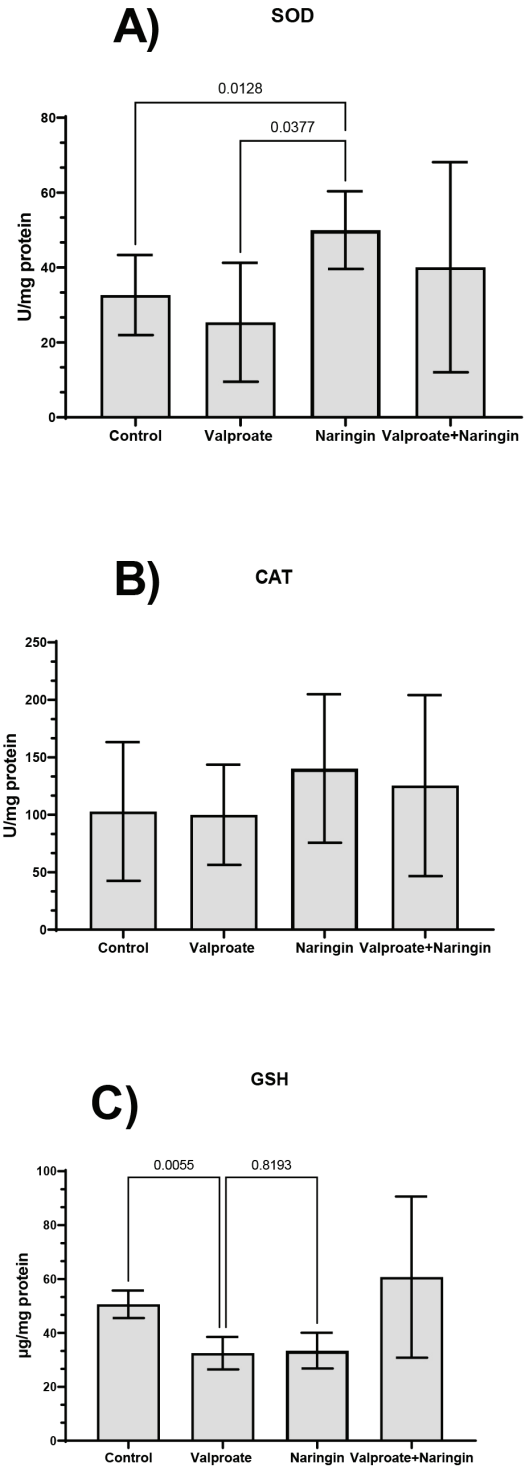

Figure 5 Liver tissue antioxidants in control mice and mice treated with daily doses of 150 mg/kg bw valproate, 25 mg/kg bw naringin, and their combination for 10 days. The numbers above bars represent statistically significant differences ($p<0.05$) between specific groups. SOD – total superoxide dismutase activity; CAT – catalase activity; GSH – reduced glutathione

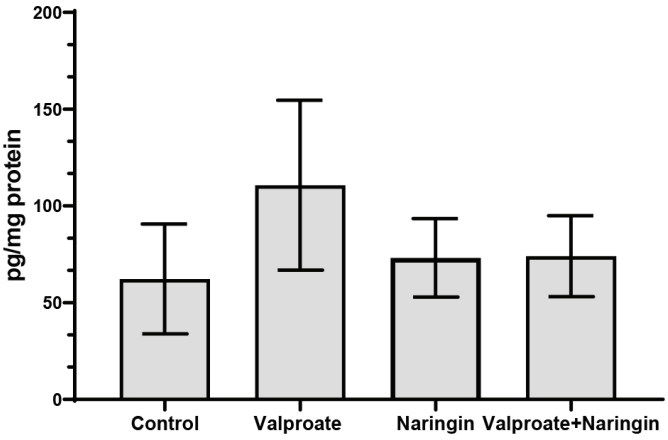

Figure 6 Transcription factor Nrf2 in the liver of control mice and mice treated with daily doses of 150 mg/kg bw valproate, 25 mg/kg bw naringin, and their combination for 10 days. No significant differences were observed between the groups

Particularly indicative was high serum glucose in the valproate plus naringin group (Table 1). Such elevation points to a possibility that the increase in lipid levels may be owed to hyperglycaemia through *de novo* lipid synthesis in the pyruvate-acetyl CoA cycle (10).

Besides the described effects, valproate and naringin, alone or in combination, did not significantly affect serum HDL and VLDL cholesterol, liver protein carbonylation, or the Nrf2 transcription factor. Nevertheless, naringin did modulate and restore crucial hepatic markers (ACOX1, PPAR-alpha, and PGC-1 alpha) of lipid metabolism and oxidative stress to near control values and certainly has a potential for use in treatment.

The main limitation of this study is that it was done in experimental animals and our findings remain to be confirmed in human trials. Future studies, non-clinical or clinical, should also include parallel monitoring of key markers of both mitochondrial and peroxisome lipid oxidation pathways. Furthermore, a combination with statins, as a few recent experimental approaches suggest (49), might elucidate naringin's role in other valproate metabolic and obesity research models.

CONCLUSION

What protective effects of naringin against valproate we found may be due to naringin restoring PPAR-alpha, PGC-1 alpha, and ACOX1 liver levels to normal. Another protective mode of naringin action we established was through increased SOD activity. We therefore believe that it deserves further investigation in combination with valproate that may shed more light on the complex interaction between regulators of lipid metabolism in the peroxisome.

Acknowledgments

We wish to dedicate this article to the memory of our dearest histology technician Ms Zrinka Benčina. Thank you Zrinka for everything you have done for us and your lab over the last 20 years.

This work was funded through the collaborative project BIOCIDI (Grant No. 106-F15-00032) of the Croatian Ministry of Health and Zagreb University Faculty of Science.

REFERENCES

1. Singh D, Gupta S, Verma I, Morsy MA, Nair AB, Ahmed AF. Hidden pharmacological activities of valproic acid: A new insight. Biomed Pharmacother 2021;142:112021. doi: 10.1016/j.biopha.2021.112021
2. Pitt B, Sutton NR, Wang Z, Goonewardena SN, Holinstat M. Potential repurposing of the HDAC inhibitor valproic acid for patients with COVID-19. Eur J Pharmacol 2021;898:173988. doi: 10.1016/j.ejphar.2021.173988
3. Đikić D, Jutrić D, Dominko K. The dual nature of the antiepileptic drug valproic acid, with possible beneficial effects in Alzheimer's disease. SEEMEDJ 2017;1:74–89. doi: 10.26332/seemedj.v1i1.26
4. NCBI. LiverTox: Clinical and Research Information on Drug-Induced Liver Injury [Internet] [displayed 31 July 2020]. Available at https://www.ncbi.nlm.nih.gov/books/NBK548284/
5. Chaudhary S, Ganjoo P, Raiusddin S, Parvez S. Nephroprotective activities of quercetin with potential relevance to oxidative stress induced by valproic acid. Protoplasma 2015;252:209–17. doi: 10.1007/s00709-014-0670-8
6. Celik E, Tunali S, Gezginci-Oktayoglu S, Bolkent S, Can A, Yanardag R. Vitamin U prevents valproic acid-induced liver injury through supporting enzymatic antioxidant system and increasing hepatocyte proliferation triggered by inflammation and apoptosis. Toxicol Mech Methods 2021;31:600–8. doi: 10.1080/15376516.2021.1943089
7. Salimi A, Alyan N, Akbari N, Jamali Z, Pourahmad J. Selenium and L-carnitine protects from valproic acid-Induced oxidative stress and mitochondrial damages in rat cortical neurons. Drug Chem Toxicol 2020;1–8. [Online ahead of print] doi: 10.1080/01480545.2020.1810259
8. Shirani K, Yousefsani BS, Shirani M, Karimi G. Protective effects of naringin against drugs and chemical toxins induced hepatotoxicity: A review. Phytother Res 2020;34:1734–44. doi: 10.1002/ptr.6641
9. Koroglu OF, Gunata M, Vardi N, Yildiz A, Ates B, Colak C, Tanriverdi LH, Parlakpinar H. Protective effects of naringin on valproic acid-induced hepatotoxicity in rats. Tissue Cell 2021;72:101526. doi: 10.1016/j.tice.2021.101526
10. Zhang X, Zhang Y, Gao W, Guo Z, Wang K, Liu S, Duan Z, Chen Y. Naringin improves lipid metabolism in a tissue-engineered liver model of NAFLD and the underlying mechanisms. Life Sci 2021;277:119487. doi: 10.1016/j.lfs.2021.119487
11. Syed AA, Reza MI, Shafiq M, Kumariya S, Singh P, Husain A, Hanif K, Gayen JR. Naringin ameliorates type 2 diabetes mellitus-induced steatohepatitis by inhibiting RAGE/NF-κB mediated mitochondrial apoptosis. Life Sci 2020;257:118118. doi: 10.1016/j.lfs.2020.118118
12. Committee for the Update of the Guide for the Care and Use of Laboratory Animals. Guide for the Care and Use of Laboratory Animals. 8th ed. Washington (DC): National Academies Press; 2011.
13. Friedewald WT, Levy RI, Fredrickson DS. Estimation of the concentration of low-density lipoprotein cholesterol in plasma, without use of the preparative ultracentrifuge. Clin Chem 1972;18:499–502. doi: 10.1093/clinchem/18.6.499
14. Oršolić N, Landeka Jurčević I, Đikić D, Rogić D, Odeh D, Balta V, Perak Junaković E, Terzić S, Jutrić D. Effect of propolis on diet-induced hyperlipidemia and atherogenic indices in mice. Antioxidants (Basel) 201;8:156. doi: 10.3390/antiox8060156
15. Đikić D, Landeka I, Knežević F, Mojsović-Ćuić A, Benković V, Horvat-Knežević A, Lončar G, Teparić R, Rogić D. Carbendazim impends hepatic necrosis when combined with imazalil or cypermethrin. Basic Clin Pharmacol Toxicol 2012;110:433–40. doi: 10.1111/j.1742-7843.2011.00831.x
16. Lowry OH, Rosebrough NJ, Farr AL, Randall RJ. Protein measurement with the Folin phenol reagent. J Biol Chem 1951;193:265–75. doi: 10.1016/S0021-9258(19)52451-6
17. Landeka Jurčević I, Dora M, Guberović I, Petras M, Rimac S, Brnčić, Đikić D. Polyphenols from wine lees as a novel functional bioactive compound in the protection against oxidative stress and hyperlipidaemia. Food Technol Biotechnol 2017;55:109–16. doi: 10.17113/ftb.55.01.17.4894
18. Nagababu E, Rifkind JM, Boindala S, Nakka L. Assessment of antioxidant activity of eugenol *in vitro* and *in vivo*. Methods Mol Biol 2010;610:165–80. doi: 10.1007/978-1-60327-029-8_10
19. Mu H, Zhou Q, Yang R, Zeng J, Li X, Zhang R, Tang W, Li H, Wang S, Shen T, Huang X, Dou L, Dong J. Naringin attenuates high fat diet induced non-alcoholic fatty liver disease and gut bacterial dysbiosis in mice. Front Microbiol 2020;11:585066. doi: 10.3389/fmicb.2020.585066
20. Bellringer ME, Rahman K, Coleman R. Sodium valproate inhibits the movement of secretory vesicles in rat hepatocytes. Biochem J 1988;249:513–9. doi: 10.1042/bj2490513
21. Grünig D, Szabo L, Marbet M, Krähenbühl S. Valproic acid affects fatty acid and triglyceride metabolism in HepaRG cells exposed to fatty acids by different mechanisms. Biochem Pharmacol 2020;177:113860. doi: 10.1016/j.bcp.2020.113860
22. Lee MH, Hong I, Kim M, Lee BH, Kim JH, Kang KS, Kim HL, Yoon BI, Chung H, Kong G, Lee MO. Gene expression profiles of murine fatty liver induced by the administration of valproic acid. Toxicol Appl Pharmacol 2007;220:45–59. doi: 10.1016/j.taap.2006.12.016
23. Ma L, Wang Y, Chen X, Zhao L, Guo Y. Involvement of CYP2E1-ROS-CD36/DGAT2 axis in the pathogenesis of VPA-induced hepatic steatosis *in vivo* and *in vitro*. Toxicology 2020;445:152585. doi: 10.1016/j.tox.2020.152585
24. Bai X, Hong W, Cai P, Chen Y, Xu C, Cao D, Yu W, Zhao Z, Huang M, Jin J. Valproate induced hepatic steatosis by enhanced fatty acid uptake and triglyceride synthesis. Toxicol Appl Pharmacol 2017;324:12–25. doi: 10.1016/j.taap.2017.03.022
25. Aires CCP, Ijlst L, Stet F, Prip-Buus C, de Almeida IT, Duran M, Wanders RJ, Silva MF. Inhibition of hepatic carnitine palmitoyltransferase I (CPT IA) by valproyl-CoA as a possible mechanism of valproate-induced steatosis. Biochem Pharmacol 2010;79:792–9. doi: 10.1016/j.bcp.2009.10.011
26. Kim HJ, Oh GT, Park YB, Lee MK, Seo HJ, Choi MS. Naringin alters the cholesterol biosynthesis and antioxidant enzyme activities in LDL receptor-knockout mice under cholesterol fed condition. Life Sci 2004;74:1621–34. doi: 10.1016/j.lfs.2003.08.026
27. Liang H, Ward WF. PGC-1alpha: a key regulator of energy metabolism. Adv Physiol Educ 2006;30:145–51. doi: 10.1152/advan.00052.2006

28. van Raalte DH, Li M, Pritchard PH, Wasan KM. Peroxisome proliferator-activated receptor (PPAR)-alpha: a pharmacological target with a promising future. Pharm Res 2004;21:1531–8. doi: 10.1023/b:pham.0000041444.06122.8d
29. Tahri-Joutey M, Andreoletti P, Surapureddi S, Nasser B, Cherkaoui-Malki M, Latruffe N. Mechanisms mediating the regulation of peroxisomal fatty acid beta-oxidation by PPARα. Int J Mol Sci 2021;22:8969. doi: 10.3390/ijms22168969
30. Lira VA, Benton CR, Yan Z, Bonen A. PGC-1alpha regulation by exercise training and its influences on muscle function and insulin sensitivity. Am J Physiol Endocrinol Metab 2010;299:E145–61. doi: 10.1152/ajpendo.00755.2009
31. Vluggens A, Andreoletti P, Viswakarma N, Jia Y, Matsumoto K, Kulik W, Khan M, Huang J, Guo D, Yu S, Sarkar J, Singh I, Rao MS, Wanders RJ, Reddy JK, Cherkaoui-Malki M. Reversal of mouse Acyl-CoA oxidase 1 (ACOX1) null phenotype by human ACOX1b isoform. Lab Invest 2010;90:696–708. doi: 10.1038/labinvest.2010.46
32. Reddy JK, Hashimoto T. Peroxisomal beta-oxidation and peroxisome proliferator-activated receptor alpha: an adaptive metabolic system. Annu Rev Nutr 2001;21:193–230. doi: 10.1146/annurev.nutr.21.1.193
33. Aoyama T, Peters JM, Iritani N, Nakajima T, Furihata K, Hashimoto T, Gonzalez FJ. Altered constitutive expression of fatty acid-metabolizing enzymes in mice lacking the peroxisome proliferator-activated receptor alpha (PPARalpha). J Biol Chem 1998;273:5678–84. doi: 10.1074/jbc.273.10.5678
34. Vamecq J, Vallee L, Fontaine M, Lambert D, Poupaert J, Nuyts JP. CoA esters of valproic acid and related metabolites are oxidized in peroxisomes through a pathway distinct from peroxisomal fatty and bile acyl-CoA beta-oxidation. FEBS Lett 1993;322:95–100. doi: 10.1016/0014-5793(93)81545-b
35. Ponchaut S, Draye JP, Veitch K, Van Hoof F. Influence of chronic administration of valproate on ultrastructure and enzyme content of peroxisomes in rat liver and kidney. Oxidation of valproate by liver peroxisomes. Biochem Pharmacol 1991;41:1419–28. doi: 10.1016/0006-2952(91)90557-L
36. Van den Branden C, Roels F. Peroxisomal beta-oxidation and sodium valproate. Biochem Pharmacol 1985;34:2147–9. doi: 10.1016/0006-2952(85)90409-5
37. Wang Y, Nakajima T, Gonzalez FJ, Tanaka N. PPARs as metabolic regulators in the liver: lessons from liver-specific PPAR-null mice. Int J Mol Sci 2020;21:2061. doi: 10.3390/ijms21062061
38. McMullen PD, Bhattacharya S, Woods CG, Sun B, Yarborough K, Ross SM, Miller ME, McBride MT, LeCluyse EL, Clewell RA, Andersen ME. A map of the PPARα transcription regulatory network for primary human hepatocytes. Chem Biol Interact 2014;209:14–24. doi: 10.1016/j.cbi.2013.11.006
39. Varanasi U, Chu R, Huang Q, Castellon R, Yeldandi AV, Reddy JK. Identification of a peroxisome proliferator-responsive element upstream of the human peroxisomal fatty acyl coenzyme A oxidase gene. J Biol Chem 1996;271:2147–55. doi: 10.1074/jbc.271.4.2147
40. Yaacob NS, Norazmi MN, Gibson GG, Kass GE. The transcription of the peroxisome proliferator-activated receptor alpha gene is regulated by protein kinase C. Toxicol Lett 2001;125:133–41. doi: 10.1016/s0378-4274(01)00433-7
41. Ke JY, Kliewer KL, Hamad EM, Cole RM, Powell KA, Andridge RR, Straka SR, Yee LD, Belury MA. The flavonoid, naringenin, decreases adipose tissue mass and attenuates ovariectomy-associated metabolic disturbances in mice. Nutr Metab (Lond) 2015;12:1. doi: 10.1186/1743-7075-12-1
42. Dayarathne LA, Ranaweera SS, Natraj P, Rajan P, Lee YJ, Han CH. Restoration of the adipogenic gene expression by naringenin and naringin in 3T3-L1 adipocytes. J Vet Sci 2021;22:e55. doi: 10.4142/jvs.2021.22.e55
43. Zeng J, Deng S, Wang Y, Li P, Tang L, Pang Y. Specific inhibition of acyl-CoA oxidase-1 by an acetylenic acid improves hepatic lipid and reactive oxygen species (ROS) metabolism in rats fed a high fat diet. J Biol Chem 2017;292:3800–9. doi: 10.1074/jbc.M116.763532
44. Komulainen T, Lodge T, Hinttala R, Bolszak M, Pietilä M, Koivunen P, Hakkola J, Poulton J, Morten KJ, Uusimaa J. Sodium valproate induces mitochondrial respiration dysfunction in HepG2 *in vitro* cell model. Toxicology 2015;331:47–56. doi: 10.1016/j.tox.2015.03.001
45. Pourahmad J, Eskandari MR, Kaghazi A, Shaki F, Shahraki J, Fard JK. A new approach on valproic acid induced hepatotoxicity: involvement of lysosomal membrane leakiness and cellular proteolysis. Toxicol In Vitro 2012;26:545–51. doi: 10.1016/j.tiv.2012.01.020
46. Jafarian I, Eskandari MR, Mashayekhi V, Ahadpour M, Hosseini MJ. Toxicity of valproic acid in isolated rat liver mitochondria. Toxicol Mech Methods 2013;23:617–23. doi: 10.3109/15376516.2013.821567
47. Jung UJ, Kim HJ, Lee JS, Lee MK, Kim HO, Park EJ, Kim HK, Jeong TS, Choi MS. Naringin supplementation lowers plasma lipids and enhances erythrocyte antioxidant enzyme activities in hypercholesterolemic subjects. Clin Nutr 2003;22:561–8. doi: 10.1016/s0261-5614(03)00059-1
48. Demonty I, Lin Y, Zebregs YE, Vermeer MA, van der Knaap HC, Jäkel M, Trautwein EA. The citrus flavonoids hesperidin and naringin do not affect serum cholesterol in moderately hypercholesterolemic men and women. J Nutr 2010;140:1615–20. doi: 10.3945/jn.110.124735
49. Raffoul-Orozco AK, Ávila-González AE, Rodríguez-Razón CM, García-Cobian TA, Pérez-Guerrero EE, García-Iglesias T, Rubio-Arellano ED. Combination effect naringin and pravastatin in lipid profile and glucose in obese rats. Life Sci 2018;193:87–92. doi: 10.1016/j.lfs.2017.11.044

Interakcija naringina s valproatom u regulaciji dislipidemije u C57BL6 miševa

Valproat je najčešće korišten antiepileptik, čiji štetni učinci uključuju masnu jetru (steatozu) i dislipidemiju. Cilj istraživanja bio je utvrditi kako će prirodni flavonoid i antioksidans naringin u interakciji s valproatom ublažiti navedene štetne učinke. Mužjaci miševa C57BL6 bili su svakodnevno tijekom 10 dana izloženi valproatu u dozi od 150 mg/kg i naringinu u dozi od 25 mg/kg te njihovim međusobnim kombinacijama u istim dozama. Nakon pokusnog razdoblja usporedili smo razinu serumskih triglicerida, kolesterola, LDL, HDL i VLDL, jetrene markere PPAR-alfa, PGC-1 alfa, ACOX1 i Nrf2 te antioksidacijske markere SOD, CAT i GSH u jetri. Svaka je jetra analizirana histološki. Valproat je povećao parametre peroksidacije lipida i izazvao izraženu mikrovezikularnu steatozu u cijelom jetrenom lobulu u svim acinarnim zonama, ali je istodobna primjena naringina ograničila steatozu na periferiju lobula. Osim toga, naringin je uspostavio normalnu ravnotežu serumskoga kolesterola, LDL i triglicerida te jetrenih markera PPAR-alfa i PGC-1 alfa, ACOX1 i MDA. Također je povećao aktivnost SOD-a. Svi ovi nalazi upućuju na to da naringin modulira ključne regulatore metabolizma lipida i da ga treba dalje istražiti u ovome modelu, bilo samog ili u kombinaciji s drugim lijekovima ili molekulama za regulaciju lipida.

KLJUČNE RIJEČI: ACOX1; kolesterol; dislipidemija; Nrf2; PPAR-alfa; PGC-1 alfa; oksidacijski stres; transkripcijski faktori za regulaciju lipida